Int Nano Lett (2017) 7:181–186
DOI 10.1007/s40089-017-0212-4

ORIGINAL ARTICLE

Spectroscopic properties of triangular silver nanoplates immobilized on polyelectrolyte multilayer-modified glass substrates

Janice B. Rabor[1] · Koki Kawamura[1] · Daiki Muko[1] · Junichi Kurawaki[1] · Yasuro Niidome[1]

Received: 22 December 2016 / Accepted: 11 July 2017 / Published online: 15 July 2017

Abstract Fabrication of surface-immobilized silver nanostructures with reproducible plasmonic properties by dip-coating technique is difficult due to shape alteration. To address this challenge, we used a polyelectrolyte multilayer to promote immobilization of as-received triangular silver nanoplates (TSNP) on a glass substrate through electrostatic interaction. The substrate-immobilized TSNP were characterized by absorption spectrophotometry and scanning electron microscopy. The bandwidth and peak position of localized surface plasmon resonance (LSPR) bands can be tuned by simply varying the concentration of the colloidal solution and immersion time. TSNP immobilized from a higher concentration of colloidal solution with longer immersion time produced broadened LSPR bands in the near-IR region, while a lower concentration with shorter immersion time produced narrower bands in the visible region. The shape of the nanoplates was retained even at long immersion time. Analysis of peak positions and bandwidths also revealed the point at which the main species of the immobilization had been changed from isolates to aggregates.

Keywords Triangular silver nanoplates · Surface-immobilized nanoplates · LSPR

✉ Janice B. Rabor
jbrabor@sci.kagoshima-u.ac.jp

[1] Department of Chemistry and Bioscience, Graduate School of Science and Engineering, Kagoshima University, 1-21-35 Korimoto, Kagoshima 890-0065, Japan

Introduction

Silver nanostructures have gained considerable interest because of their potential applications in plasmonic imaging and sensing [1–5]. These applications depend on the nanostructure's localized surface plasmon resonance (LSPR) properties such as band position, bandwidth, and magnitude. One way to control these properties is to change the shape of the nanostructure. For example, recent studies [6–9] have suggested that anisotropic silver nanostructures are better than isotropic nanoparticles for plasmonic applications. Strong plasmon coupling, which occurs in regions called hot spots, are more pronounced at sharp edges and tips of anisotropic nanostructures than in isotropic nanoparticles [10, 11]. Triangular silver nanoplates (TSNP) are one such anisotropic silver nanostructure [10–12]. TSNP have multiple LSPR bands in visible and near-infrared (near-IR) regions that can be used to enhance the excitation and emission processes simultaneously in metal-enhanced fluorescence (MEF) [1, 13]. It can also be used to enhance scattering in surface-enhanced Raman scattering (SERS) where it was reported that highest enhancement is achieved when LSPR peak wavelength is between the wavelength of the excitation light source and that of the chosen Raman-scattered photon wavelength [14]. In order for TSNP to be effective in these applications, it is necessary to maintain its triangular shape. However, the triangular shape can be altered during aggregation [15]. Thus, it is important to control the aggregation of TSNP to prevent shape alteration.

One way to control aggregation is to immobilize TSNP on a surface. When silver nanostructures are immobilized on a substrate, the aggregation state over time is easier to maintain. Surface-immobilized silver

nanostructures have been used for SERS and MEF applications with glass [15–17], quartz [1], and polymeric substrates [18]. Modified dip-coating technique has been used to fabricate substrate-immobilized silver nanostructures, including TSNP, with desirable LSPR properties because of its simplicity [15, 17, 19–21]. Rivero et al. [16] successfully produced multicolor substrate-immobilized silver nanostructures, but their method is highly dependent on the pH of the colloidal solution. Zhang et al. [17] fabricated substrate-immobilized TSNP with tunable LSPR properties using multiple TSNP colloidal solutions with different nanoplate sizes, but the LSPR of these substrate-immobilized TSNP are only blueshifts compared to their corresponding colloidal solutions. The colloidal solutions also have to be pre-treated before the dip-coating step. Bakar et al. [15] used 3-aminopropyltrimethoxysilane as a coupling agent to immobilize TSNP to a glass substrate but longer immersion time leads to round-shaped immobilized-nanoplates. Furthermore, few hot spots are formed because TSNP are immobilized as isolates.

To address the above-mentioned challenges, we immobilized citrate-stabilized TSNP on a glass substrate modified with polyelectrolyte multilayer (PEM). The PEM promoted the immobilization of TSNP on the substrate through electrostatic interaction. In this way, the shape of TSNP was retained. We used as-received colloidal solutions without the need for pH adjustment or pre-treatment. In this paper, we correlate the spectroscopic properties of TSNP immobilized on PEM-modified substrates to its shape and state of aggregation. LSPR bands of TSNP were tuned by varying immersion parameters. Long immersion time and high concentration of colloidal solution led to redshifted and broad LSPR bands.

Experimental

Chemicals and materials

The following chemicals were used in this work: citrate-stabilized triangular silver nanoplate (TSNP) colloidal solution (AgWS5, 0.02 mg/g, Dai Nippon Toryo Co. Ltd.), poly(diallyldimethylammonium chloride) (PDDA, 20%, MW 400,000–500,000, Aldrich), and polystyrene sulfonate (PSS, MW 500,000, Scientific Polymer Products, Inc.). Deionized water (18.2 MΩ cm) was used throughout all experiments.

Glass slides (S1126, 50 × 10 × 1 mm, Matsunami) were used as substrates. Glass slides were cleaned by sonication using detergent, deionized water, and acetone in sequence. Then, they were put in a UV/ozone cleaner.

Immobilization of TSNP on a glass substrate

TSNP were immobilized on PEM-modified glass substrate by a variation of previously reported layer-by-layer technique [22]. First, a clean glass slide was modified with PEM by sequentially dipping it in cationic PDDA (2 mg/mL) and anionic PSS (2 mg/mL) solutions for 30 min each. A rinsing step in water for 1 min was performed in between the two polyelectrolyte baths. A drying step using compressed air was performed after each rinsing step. The cycle was repeated 3×. The PEM coating was completed by dipping the glass slide in PDDA solution for another 30 min. The final composition of PEM was $(PDDA\text{-}PSS)_3$-PDDA. TSNP was immobilized by immersion of the PEM-modified glass slide in an as-received TSNP colloidal solution at varying immersion time.

Higher concentration of TSNP (2× and 4×) was prepared from the as-received colloidal solution (1×, 0.02 mg/g) by centrifugation and redispersion. To get 2× and 4× colloidal solutions, 2 and 4 mL of 1× colloidal solution was each centrifuged at 5000 rpm for 30 min and then redispersed into 1 mL water, respectively.

Characterization of TSNP films

UV–Visible-NIR spectrophotometer (Jasco V-630) was used to characterize the optical properties of TSNP colloidal solution and the substrate-immobilized ones. Field emission scanning electron microscopy (SEM, Hitachi SU-70) was used to determine the shape and distribution of TSNP on the substrate.

Results and discussion

The main purpose of this work was to produce substrate-immobilized TSNP with retained triangular shape and controlled aggregation by modified layer-by-layer technique. First, we confirmed the immobilization of TSNP on PEM-modified glass substrate by comparing the extinction spectrum of TSNP colloidal solution to that of substrate-immobilized ones, as shown Fig. 1a. In this case, the TSNP were immobilized by immersing the substrate into the as-received colloidal solution for 0.5 h. The extinction spectrum of the colloidal solution showed three LSPR bands typical for triangular-shaped nanoplates [10, 11]: a strong dipole resonance band at 802 nm, a weak shoulder due to in-plane quadrupole resonance around 500 nm, and a sharp out-of-plane resonance at 332 nm. The extinction spectrum of the substrate-immobilized TSNP also showed three LSPR bands shifting to shorter wavelengths. Since a blueshift may suggest shape alteration of the nanoplates, we took SEM images. Figure 2 (1×, 0.5 h) shows that the

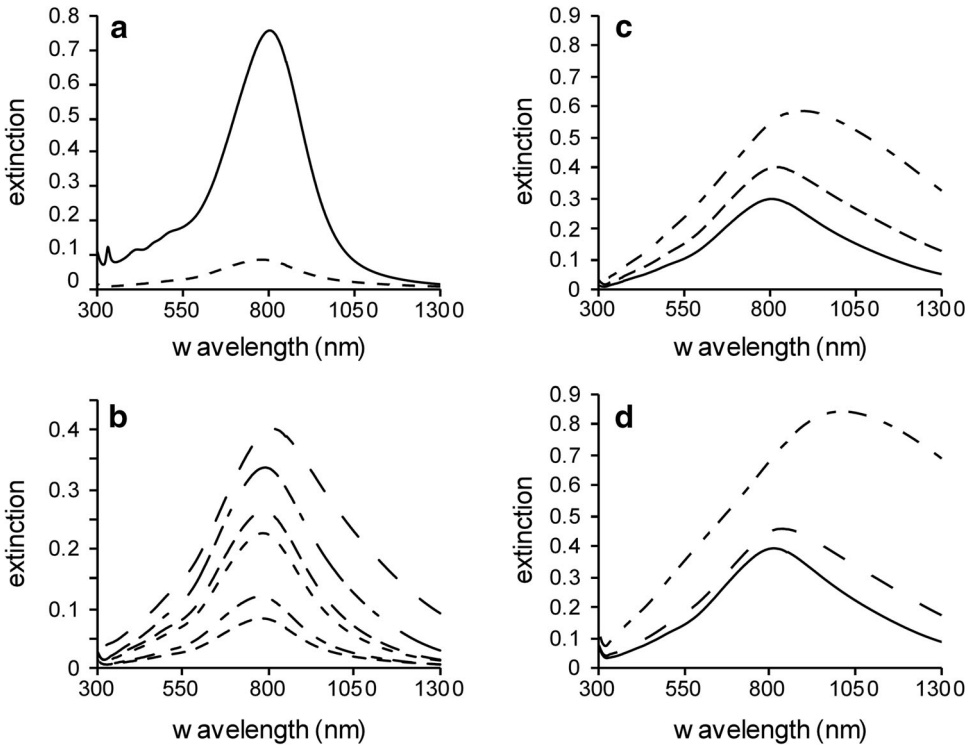

Fig. 1 Extinction spectra of **a** TSNP colloidal solution (*solid line*) and substrate-immobilized TSNP (*dotted line*); **b** substrate-immobilized TSNP from ×1 colloidal solution after various immersion times (*from bottom to top* 0.5, 1, 2, 3, 5, and 24 h); substrate-immobilized TSNP from different colloidal solution concentrations (*from bottom to top* ×1, ×2, and ×4) after **c** 5 h and **d** 24 h immersion

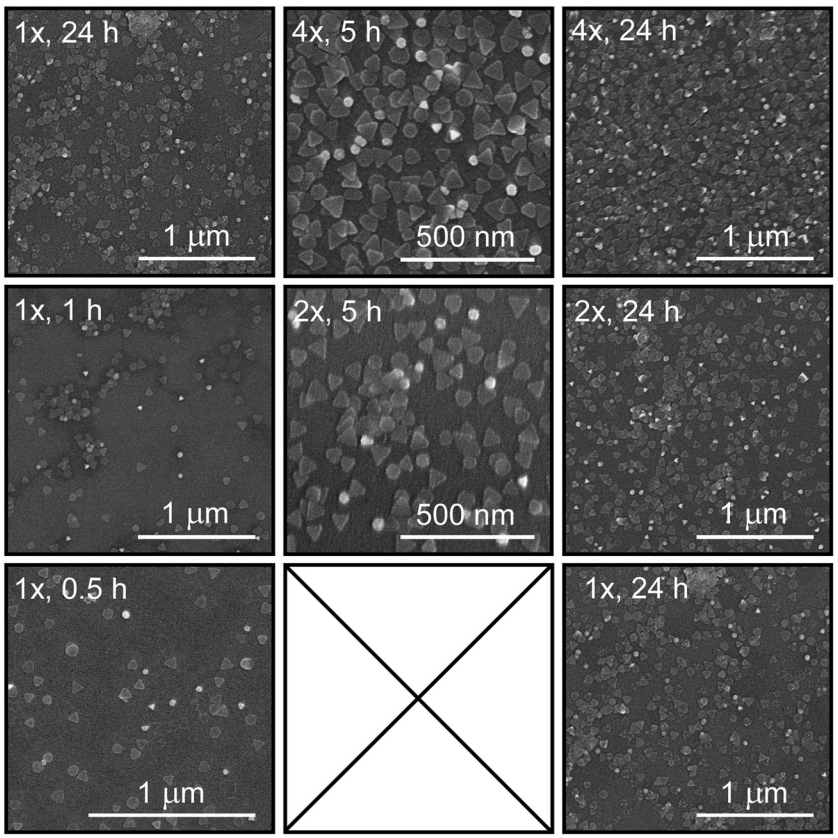

Fig. 2 SEM images of substrate-immobilized TSNP from various concentrations of colloidal solution and immersion time

nanoplates retained their triangular shape. This indicates that the blueshift was not caused by shape alteration but by decrease in refractive index experienced by TSNP on the substrate as compared in water. Thus, TSNP were successfully immobilized on PEM-modified glass substrate. Without the PEM modification, TSNP were not immobilized on a glass substrate. It can be concluded that the PEM promotes the immobilization by its electrostatic interaction with TSNP.

After confirming the immobilization of TSNP on PEM-modified glass substrate, we studied the effects of immersion time and concentration of the colloidal solution to the optical properties of the immobilized TSNP. Figure 1b shows the extinction spectra of immobilized TSNP obtained at various immersion times. The immersion times, from bottom to top, are 0.5, 1, 2, 3, 5, and 24 h. The extinction of LSPR bands increased with increasing immersion time but peak positions and bandwidths were almost retained. In comparison to the LSPR bands of the colloidal solution, immobilized TSNP using 0.5–5 h immersion showed blueshifts. To study the effect of the concentration of colloidal solution, the as-received TSNP colloidal solution was concentrated to 2× and 4× of its original concentration as detailed in the experimental section. From here on, the as-received TSNP colloidal solution is denoted as 1× colloidal solution. The extinction spectra of substrate-immobilized TSNP from these three concentrations at 5 and 24 h immersion are shown in Fig. 1c, d, respectively. As the concentration increased, the LSPR bands shifted toward longer wavelength, the bandwidth broadened, and the peak intensity increased. In 5 h immersion, only immobilized TSNP from higher concentration (2× and 4×) showed redshifted and broaden LSPR bands. While in 24 h immersion, TSNP from all three concentrations showed redshifted and broaden LSPR bands. The immobilized TSNP from 1× concentration exhibited shift to the longer wavelength by 7 nm while from 2× and 4× concentration exhibited 32 and 208 nm redshifts, respectively. Thus, longer immersion in more concentrated solutions led to increased, redshifted, and broadened LSPR bands. By simply changing the immersion time and concentration of colloidal solution, we were able to tune the peak positions and bandwidths of the LSPR bands of the immobilized TSNP. A previous study [15] also changed immersion time but they were unable to produce tunable LSPR bands.

As previously described, the extinction intensity increased with increasing colloidal concentration and immersion time. This is a consequence of the increased density of TSNP on the substrate as evidenced by the SEM images found in Fig. 2. These SEM images also show that aggregation was dominant in higher concentration of colloidal solution and 24 h immersion. What is interesting is that aggregation was also observed using 1× colloidal solution as early as 1 h immersion but this aggregation did not significantly affect the peak position or the bandwidth of the LSPR bands (see Fig. 1b). The narrow LSPR bands are typical for isolated nanoparticles. Thus, we can assign the observed LSPR bands at 1 h immersion to isolated TSNP. We also found that the shapes of the nanoplates were generally retained even in aggregation. Although nanoplates with irregular shapes were observed, the distribution of triangular nanoplates was still higher than the distribution of irregular shapes.

Zhang et al. [17] achieved LSPR peak position tunability of immobilized silver nanoplates by using multiple colloidal solutions with different nanoplate sizes. In contrast, this study used only a single colloidal solution and achieved tunability by manipulating the immersion time and concentration of the colloidal solution. This tunability is depicted in Fig. 3a where the extinction of the strongest LSPR band of each immobilized TSNP was plotted against its peak position. The plot was divided into two regions—I and II. The boundary is at 800 nm, corresponding to the strongest LSPR band of the colloidal solution. The LSPR peak positions are blueshifts in region I, while they are redshifts in region II when compared to that of the colloidal solution. This clearly demonstrates peak position tunability of the LSPR bands of our immobilized-substrates. In addition, the plot also gives insight into the relationship between the peak position and aggregation state of immobilized TSNP. In region I, the extinction increased steeply to 0.33, and the peak position changes were not

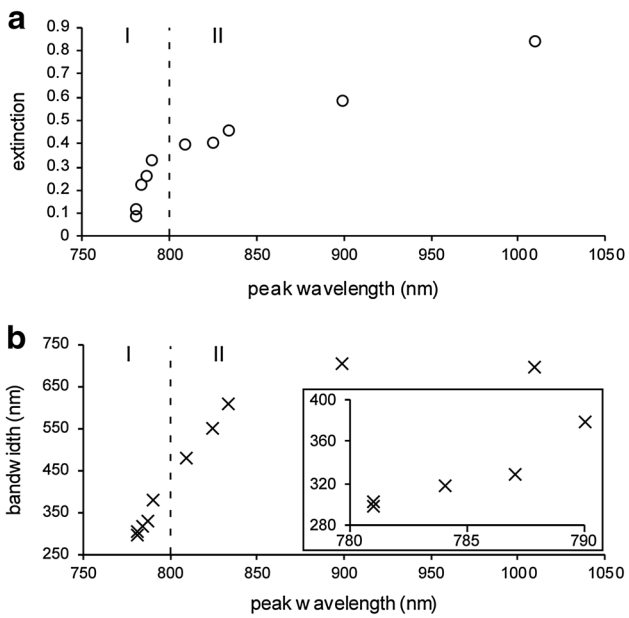

Fig. 3 Dependence of LSPR **a** extinction intensity and **b** bandwidth to its peak position; bandwidths are expressed as full-width at half-maximum

significant. This indicates that well-isolated TSNP were dominantly immobilized on the substrate in region I. In region II, the extinction showed gradual increase and the peak positions showed large redshifts. This indicates aggregation of the TSNP on the substrate in region II. These statements are consistent with the SEM images found in Fig. 2.

The LSPR bandwidth tunability is also important. The bandwidth of the strongest LSPR band was plotted against its peak position in Fig. 3b. Here, the bandwidth is expressed as full-width at half-maximum (fwhm). When the peak positions were shorter than 790 nm, the changes in bandwidth were limited (300–330 nm, see inset). The narrow bandwidths indicate preservation of isolated TSNP. On the other hand, the bandwidth changed significantly when the peak positions were longer than 790 nm. This indicates aggregation of TSNP. The peak position at 790 nm suggests that the main species on the substrate were isolated TSNP (see Fig. 3a), but the broadened bandwidth (378 nm) also suggests that the nanoplate aggregation is initiated. When the peak positions were longer than 790 nm, the large bandwidth (480–700 nm) indicates the presence of aggregated TSNP. Thus, the main species of immobilization is changed from isolates to aggregates at 790 nm with an extinction of 0.33 and a bandwidth of 330 nm. This corresponds to an immersion time of 5 h using 1× colloidal solution. These immobilization features are different from previous studies [15–17].

Conclusions

TSNP were successfully immobilized on PEM-modified glass substrate using layer-by-layer technique. The method was simple; we used as-received colloidal solutions without pH adjustment or pre-treatment. The bandwidth and peak position of LSPR bands can be tuned by simply varying the concentration of the colloidal solution and immersion time. TSNP immobilized from higher concentration of colloidal solution and longer immersion time produced broadened LSPR bands in the near-IR region, while lower concentration and shorter immersion time produced narrower bands in the visible region. More aggregated TSNP showed broader and redshifted LSPR. The point at which the main species of nanoplate immobilization had been changed from isolates to aggregates was revealed by the analysis of LSPR peak positions and bandwidths. The features of our immobilized TSNP are very different from those in the previous works [15–17], but have tunable peak positions and bandwidths. The immobilized TSNP obtained in this study should be explored in various plasmonic applications such as Raman scattering, fluorescence applications, and photoenergy conversion processes.

Acknowledgements This work was supported in part by a KAKENHI Grant-in-Aid for Challenging Exploratory Research (No. 15K13729), and the Nanotechnology Platform Programs (Molecule and Material Synthesis and Advanced Characterization Platform) from the Ministry of Education, Culture, Sports, Science and Technology (MEXT), Japan.

References

1. Geddes, C.D., Gryczynski, I., Malicka, J., Gryczynski, Z., Lakowicz, J.R.: Metal-enhanced fluorescence: potential applications in HTS. Comb. Chem. High Throughput Screen. **6**, 109–117 (2003)
2. Moskovits, M.: Surface-enhanced Raman spectroscopy: a brief retrospective. J. Raman Spectrosc. **36**, 485–496 (2005). doi:10.1002/jrs.1362
3. Pelton, M., Bryant, G.W.: Introduction to metal-nanoparticle plasmonics. Wiley, Chichester (2013)
4. Xia, Y.: Optical sensing and biosensing based on non-spherical noble metal nanoparticles. Anal. Bioanal. Chem. **408**, 2813–2825 (2016). doi:10.1007/s00216-015-9203-3
5. Qin, X., Luo, Y., Lu, W., Chang, G., Asiri, A.M., Al-Youbi, A.O., Sun, X.: One-step synthesis of Ag nanoparticles-decorated reduced graphene oxide and their application for H_2O_2 detection. Electrochim. Acta **79**, 46–51 (2012). doi:10.1016/j.electacta.2012.06.062
6. Aslan, K., Lakowicz, J.R., Geddes, C.D.: Metal-enhanced fluorescence using anisotropic silver nanostructures: critical progress to date. Anal. Bioanal. Chem. **382**, 926–933 (2005). doi:10.1007/s00216-005-3195-3
7. Millstone, J.E., Hurst, S.J., Métraux, G.S., Cutler, J.I., Mirkin, C.A.: Colloidal gold and silver triangular nanoprisms. Small **5**, 646–664 (2009). doi:10.1002/smll.200801480
8. Yuan, H., Fales, A.M., Khoury, C.G., Liu, J., Vo-Dinh, T.: Spectral characterization and intracellular detection of surface-enhanced Raman scattering (SERS)-encoded plasmonic gold nanostars: nanostars SERS characterization. J. Raman Spectrosc. **44**, 234–239 (2013). doi:10.1002/jrs.4172
9. Pastoriza-Santos, I., Alvarez-Puebla, R.A., Liz-Marzán, L.M.: Synthetic routes and plasmonic properties of noble metal nanoplates. Eur. J. Inorg. Chem. **2010**, 4288–4297 (2010). doi:10.1002/ejic.201000575
10. Jin, R., Cao, Y.C., Hao, E., Métraux, G.S., Schatz, G.C., Mirkin, C.A.: Controlling anisotropic nanoparticle growth through plasmon excitation. Nature **425**, 487–490 (2003). doi:10.1038/nature02020
11. Sherry, L.J., Jin, R., Mirkin, C.A., Schatz, G.C., Van Duyne, R.P.: Localized surface plasmon resonance spectroscopy of single silver triangular nanoprisms. Nano Lett. **6**, 2060–2065 (2006). doi:10.1021/nl061286u
12. Kelly, J.M., Keegan, G., Brennan-Fournet, M.E.: Triangular silver nanoparticles: their preparation, functionalisation and

properties. Acta Phys. Pol. A **122**, 337–345 (2012). doi:10.12693/APhysPolA.122.337
13. Geddes, C.D., Lakowicz, J.R.: Editorial: metal-enhanced fluorescence. J. Fluoresc. **12**, 121–129 (2002). doi:10.1023/A:1016875709579
14. Sharma, B., Fernanda Cardinal, M., Kleinman, S.L., Greeneltch, N.G., Frontiera, R.R., Blaber, M.G., Schatz, G.C., Duyne, V.P.R.: High-performance SERS substrates. MRS Bull. (2013). doi:10.1557/mrs.2013.161
15. Bakar, N.A., Shapter, J.G., Salleh, M.M., Umar, A.A.: Self-assembly of high density of triangular silver nanoplate films promoted by 3-aminopropyltrimethoxysilane. Appl. Sci. **5**, 209–221 (2015). doi:10.3390/app5030209
16. Rivero, P.J., Goicoechea, J., Urrutia, A., Matias, I.R., Arregui, F.J.: Multicolor layer-by-layer films using weak polyelectrolyte assisted synthesis of silver nanoparticles. Nanoscale Res. Lett. **8**, 1–10 (2013)
17. Zhang, X.-Y., Hu, A., Zhang, T., Lei, W., Xue, X.-J., Zhou, Y., Duley, W.W.: Self-assembly of large-scale and ultrathin silver nanoplate films with tunable plasmon resonance properties. ACS Nano **5**, 9082–9092 (2011). doi:10.1021/nn203336m
18. Aslan, K., Holley, P., Geddes, C.D.: Metal-enhanced fluorescence from silver nanoparticle-deposited polycarbonate substrates. J. Mater. Chem. **16**, 2846 (2006). doi:10.1039/b604650a
19. Ray, A., Kopelman, R., Chon, B., Briggman, K., Hwang, J.: Scattering based hyperspectral imaging of plasmonic nanoplate clusters towards biomedical applications: hyperspectral imaging of plasmonic nanoplates. J. Biophotonics. (2015). doi:10.1002/jbio.201500177
20. Zhang, C.-H., Zhu, J., Li, J.-J., Zhao, J.-W.: Focus and enlarge the enhancement region of local electric field by overlapping Ag triangular nanoplates. Eur. Phys. J. Appl. Phys. **73**, 10501 (2016). doi:10.1051/epjap/2015150404
21. Lu, W., Luo, Y., Chang, G., Liao, F., Sun, X.: Layer-by-layer self-assembly of multilayer films of polyelectrolyte/Ag nanoparticles for enzymeless hydrogen peroxide detection. Thin Solid Films **520**, 554–557 (2011). doi:10.1016/j.tsf.2011.06.085
22. Decher, G., Hong, J.D., Schmitt, J.: Buildup of ultrathin multilayer films by a self-assembly process: III. Consecutively alternating adsorption of anionic and cationic polyelectrolytes on charged surfaces. Thin Solid Films **210**, 831–835 (1992). doi:10.1016/0040-6090(92)90417-A